滋賀大学教育学部紀要
No. 66, pp. 119-133, 2016

Chemical Study of Precipitation by Lake Biwa at Otsu, Shiga, Japan
— II. Trends of Chemical Compositions from 1991 to 2009 —

Yoshihiro MIZUKAMI* and Munetsugu KAWASHIMA**

Abstract

Precipitation samples by Lake Biwa at Otsu, Shiga Prefecture, Japan, collected over a 19 year period, from January 1991 to December 2009, were analyzed. Dissolved ions, including H^+, NH_4^+, Na^+, K^+, Mg_2^+, Ca_2^+, Cl^-, NO_3^- and SO_4^{2-}, were analyzed in 1818 samples. The pH of these samples ranged from 3.3 to 7.3, with an average of 4.59. Trends in chemical components of precipitation over the 19 year period were determined, with origins of dissolved ions deduced by principal components analysis. Deposition of $[H^+]$ according to rainfall shows characteristic distribution, due to the deposition balance among $[NO_3^-]$, $[SO_4^{2-}]$, $[NH_4^+]$ and $[Ca^{2+}]$.

Key words: Wet deposition, Dissolved ions, Trends over 19 years, Principal components analysis, Acidification

Introduction

Acid rain is a global environmental problem, requiring long-term monitoring of precipitation. For example, the chemical composition of precipitation in rural France and at other sites has been reported (Sicard et al., 2007 and references therein).

Otsu is a city located on the shore of Lake Biwa in Shiga Prefecture, Japan. Otsu is situated near major metropolitan areas including Kyoto, Osaka and Kobe, all of which are large cities, with many industrial plants and heavy vehicular traffic. Precipitation at Otsu is thought to be influenced not only by long range transport components but by local sources.

Ions and nutrients in precipitation at Lake Biwa can affect the environment. The chemical composition of precipitation samples obtained at Otsu can provide clues to their origin and environmental impact. We previously analyzed precipitation samples obtained by Lake Biwa from December 1990 to November 1994 (Mizukami et al. 1994). This study extends those results, by analyzing precipitation samples obtained over 19 years, from January 1991 to December 2009. The concentrations of H^+ and other dissolved ions in precipitation were analyzed. Trends in precipitation were determined and the origins of these ions deduced by principal component analysis. We also corrected for sea-salt, using not only Na^+ but other ions as standard ions. The distribution of $[H^+]$ deposition as a function of rainfall may provide important insights into the course of acidification.

* Faculty of Education, Shiga University
** Professor Emeritus, Shiga University

Experimental

Sampling and chemical analysis

Precipitation samples over 24 hours were collected at fixed times from January 1991 to December 2009 in polyethylene tanks, using funnels 290 mm in diameter, at a site located on the Ishiyama Campus of Shiga University (34° 56'57"N, 135° 54'18"E), Otsu, Shiga Prefecture, Japan (Fig. 1). Precipitation samples of rainfall above 0.3 mm were selected and analyzed.

Water samples were filtered with Membrane filters (Ultipore 0.20 μm) in the laboratory at room temperature. Snow samples were filtered after melting at room temperature. The pH of each sample was measured with a pH meter (HORIBA H-7LD or B-112), and its conductivity at 25℃ was measured with a conductivity meter (HORIBA C-172). The filtered samples were frozen and stored in polyethylene bottles at −20℃ until tested. Samples were subsequently analyzed by ion exchange chromatography.

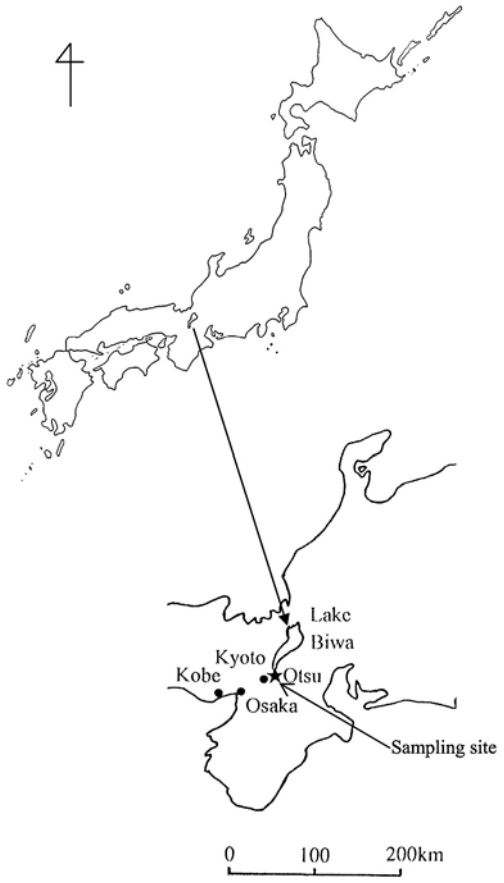

Fig. 1 Location of the sampling site

Principal components analysis

Principal components analysis is widely used for multivariate statistical analysis. In this study, the concentrations of H^+, NH_4^+, Na^+, K^+, Mg^{2+}, Ca^{2+}, Cl^-, NO_3^- and SO_4^{2-} were standardized and a correlation matrix obtained. This matrix was diagonalized to obtain eigenvalues and eigenvectors. Several eigenvectors (principal components) with large eigenvalues were used to interpret the characteristics of variables. Each principal component was a linear combination of variables. Variables were constructed from the concentration of each dissolved ion. The vector components of eigenvector (factor loading value) for each principal component were used to characterize each variable.

Results and Discussion

Rainfall by months compared with AMeDAS and ionic balance by months

Table 1 summarizes the number of samples obtained during each year and month. A maximum of 118 samples was obtained during 1993 and a minimum of 58 in 2002. Monthly groupings showed that a maximum of 199 samples were obtained in June and a minimum of 106 in November.

An Automated Meteorological Data Acquisition System (AMeDAS) is located at 34° 59' 30"N, 135° 54'42"E), 4.5 km north of our sampling site. An AMeDAS is a high-resolution automated surface observation station for gathering regional weather data, including wind direction and speed, amounts of precipitation, temperature, humidity, and atmospheric

Table 1 Number of samples.

	Jan	Feb	Mar	Apr	May	June	July	Aug	Sep	Oct	Nov	Dec	Sum
1991	9	8	12	13	6	12	15	3	9	13	5	6	111
1992	4	6	13	11	14	7	9	10	4	5	7	9	99
1993	9	8	7	10	8	13	15	12	12	6	9	9	118
1994	9	11	7	6	10	10	4	4	12	5	3	9	90
1995	6	4	12	15	15	9	16	3	8	5	4	5	102
1996	5	3	11	7	6	16	6	7	9	9	7	5	91
1997	5	5	8	9	12	9	12	4	10	3	10	6	93
1998	7	9	8	11	9	11	5	8	10	12	2	4	96
1999	5	6	4	10	6	11	5	7	9	5	2	0	70
2000	6	2	6	8	11	15	6	3	12	10	6	4	89
2001	6	5	10	4	6	6	2	5	5	5	2	4	60
2002	3	2	4	4	7	5	6	3	5	7	4	8	58
2003	6	4	8	15	8	14	17	13	9	5	9	3	111
2004	3	4	7	9	12	11	7	11	12	11	5	4	96
2005	6	7	11	8	7	11	13	12	7	9	3	4	98
2006	9	9	13	10	12	6	16	5	8	8	5	11	112
2007	7	8	5	10	11	9	15	5	8	6	7	8	99
2008	10	9	14	10	6	13	8	8	9	7	7	8	109
2009	9	11	9	8	11	11	16	7	5	10	9	10	116
Sum	124	121	169	178	177	199	193	130	163	141	106	117	1818

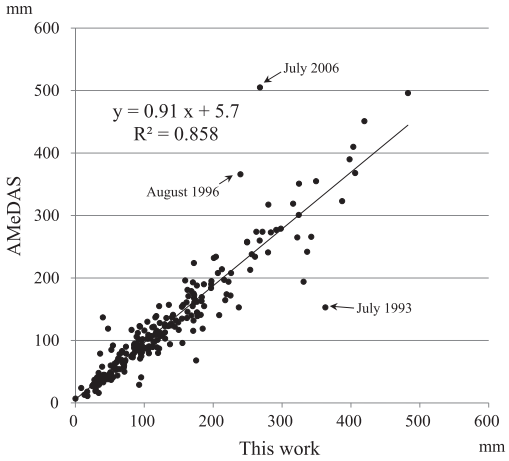

Fig. 2 Rainfall by months compared with data from AMeDAS

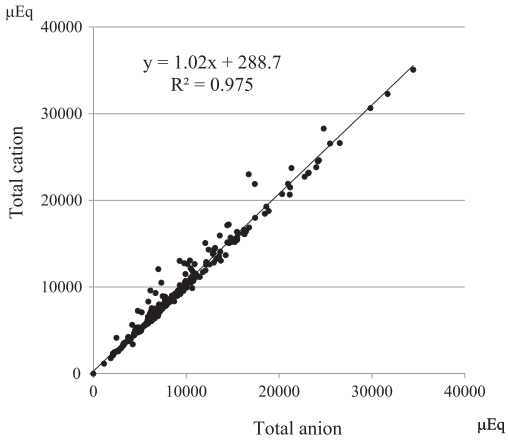

Fig. 3 Plots of the total anion depositions vs. the total cation depositions by months

pressure. A comparison of our monthly rainfall data with those of AMeDAS (Fig. 2) generally showed good correlations (slope ; 0.91, R^2 = 0.858), except for three months, July 1993, August 1996, and July 2006. Exclusion of those three months resulted in improved correlation (slope, 0.92 ; R^2 =0.922). AMeDAS readings may be erroneous (Iida, 2006), although that it unlikely because AMeDAS is an automated system. We also observed ionic balance, defined as a balance between deposition of all anions and cations by month (slope, 1.02 ; R^2= 0.975 ; Fig. 3).

Frequency distribution of pH and sea-salt correction

Figure 4 shows the frequency distribution of pH values. The pH of precipitation samples ranged from 3.3 to 7.3, with a long tail for higher pH. The simple arithmetic average pH was 4.59. Table 1 shows that the volume-weighted average of [H^+] over 19 years was 30.7 μEq/l, with a corresponding pH of 4.51. If precipitation of pH <5.0 is defined as "acid rain", then 1479 (81%) of the 1818 samples obtained over the 19 period were acid rain. Our previous study reported that 89% of the precipitation samples obtained at Otsu through the end of 1993 were considered acid rain (Mizukami et al. 1994). Thus, the acidity of precipitation at Otsu has declined over the past 16 years.

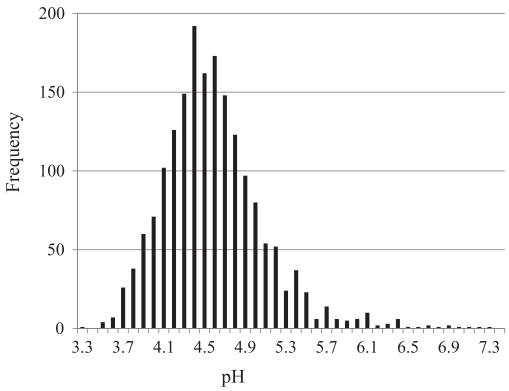

Fig. 4 Frequency distribution of pH for 1818 samples from January 1991 to December 2009

As previously described (Mizukami et al. 1994), we corrected for sea-salt using not only Na^+ but other ions as standard ions. To ensure that non sea-salt portions of other ions have positive concentrations, [Na^+], [Mg^{2+}], [K^+], [Ca^{2+}] and [Cl^-] were used as standard ions for sea-salt correction in 825, 606, 145, 32 and 210 samples, respectively.

Annual trends from 1991 to 2009 and average monthly variation

Volume-weighted annual mean concentrations of H^+, NO_3^- and SO_4^{2-} and rainfall from 1991 to 2009 are shown in Fig. 5. Total rainfall was highest in 1993 and lowest in 1994. SO_4^{2-} concentration peaked in 2001 and 2002, which may have been due to the emission of SO_2 gas by a volcano in 2000 as discussed later. NO_3^- concentration peaked in 2003.

Volume-weighted annual mean concentrations of H^+, NH_4^+, Na^+, K^+, Mg^{2+}, Ca^{2+}, Cl^-, NO_3^- and SO_4^{2-} from 1991 to 2009 are summarized in Table 2. The arithmetic averages, coefficients of variation (CVs) and volume-

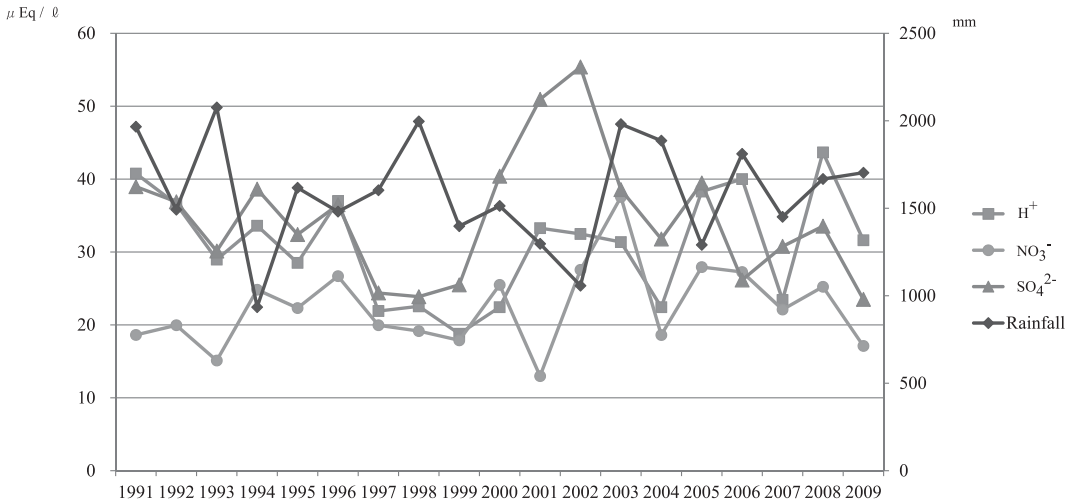

Fig. 5 Volume-weighted annual mean concentrations of H^+, NO_3^-, SO_4^{2-} and rainfall for 19 years

Table 2 Rainfall, pH and volume-weighted annual mean concentrations of dissolved ion from 1991 to 2009 (nss means non sea-salt)

Year	Rainfall (mm)	pH	H^+ (μEq/ℓ)	NH_4^+ (μEq/ℓ)	Na^+ (μEq/ℓ)	Na^+ (nss) (μEq/ℓ)	K^+ (μEq/ℓ)	K^+(nss) (μEq/ℓ)	Mg^{2+} (μEq/ℓ)	Mg^{2+} (nss) (μEq/ℓ)	Ca^{2+} (μEq/ℓ)	Ca^{2+} (nss) (μEq/ℓ)	Cl^- (μEq/ℓ)	Cl^-(nss) (μEq/ℓ)	NO_3^- (μEq/ℓ)	SO_4^{2-} (μEq/ℓ)	SO_4^{2-} (nss) (μEq/ℓ)
1991	1966.3	4.40	40.8	14.7	12.5	2.6	3.4	3.1	2.8	0.5	6.5	6.1	22.6	11.1	18.6	39.0	37.8
1992	1492.1	4.41	36.6	14.6	10.6	3.3	2.0	1.8	2.2	0.5	7.9	7.5	16.1	7.6	20.0	36.9	36.0
1993	2076.3	4.52	29.0	11.9	7.9	1.7	1.7	1.6	1.7	0.3	7.3	7.0	13.8	6.6	15.1	30.1	29.4
1994	934.8	4.59	33.6	15.9	12.3	4.7	2.7	2.5	2.6	0.9	11.4	11.1	14.4	5.6	24.8	38.6	37.7
1995	1617.0	4.56	28.5	18.6	9.1	1.4	2.0	1.8	2.9	1.1	9.7	9.4	14.5	5.5	22.3	32.4	31.5
1996	1480.6	4.57	37.0	20.4	11.8	3.3	2.8	2.7	3.0	1.1	12.9	12.5	19.0	9.2	26.7	36.5	35.5
1997	1603.1	4.63	21.9	14.7	8.8	1.7	1.1	1.0	2.8	1.2	9.5	9.2	14.2	6.1	20.0	24.4	23.5
1998	1996.5	4.70	22.5	13.6	6.1	1.3	1.3	1.2	2.8	1.7	9.2	9.0	11.4	5.9	19.1	23.9	23.3
1999	1397.7	4.87	18.8	13.3	11.1	1.3	2.0	1.7	3.6	1.3	12.5	12.1	16.5	5.2	17.9	25.5	24.3
2000	1513.3	4.83	22.4	23.8	16.0	2.5	2.3	2.1	6.5	3.4	27.6	27.1	26.3	10.8	25.5	40.4	38.8
2001	1297.0	4.71	33.3	7.1	14.5	1.1	2.3	2.1	7.6	4.5	27.8	27.2	25.6	10.1	13.0	50.9	49.4
2002	1057.5	4.66	32.5	15.4	20.7	1.8	3.2	2.8	10.3	6.0	32.6	31.8	28.9	7.1	27.5	55.4	53.1
2003	1980.9	4.58	31.4	20.2	13.4	3.6	1.8	1.6	7.8	5.7	26.9	26.5	20.0	8.8	37.5	38.6	37.4
2004	1886.3	4.73	22.4	12.9	14.8	9.3	1.0	0.9	4.5	3.2	18.5	18.3	17.8	11.4	18.6	31.8	31.1
2005	1290.8	4.54	38.3	17.5	13.1	4.6	2.6	2.4	4.0	2.0	15.2	14.8	17.2	7.3	27.9	39.5	38.4
2006	1811.2	4.50	40.0	15.0	12.2	3.5	4.1	3.9	11.3	9.3	8.3	7.9	25.0	15.0	27.3	26.2	25.1
2007	1450.7	4.74	23.4	16.7	14.8	5.7	3.3	3.1	7.2	5.2	16.1	15.7	16.0	5.5	22.1	30.8	29.7
2008	1667.3	4.42	43.7	11.8	13.3	5.6	1.7	1.6	4.4	2.6	13.6	13.2	22.4	13.4	25.2	33.5	32.6
2009	1703.1	4.48	31.6	8.2	9.5	5.6	1.2	1.1	2.2	1.3	7.7	7.5	17.5	12.9	17.1	23.5	23.0
average	1590.7	4.60	30.9	15.1	12.2	3.4	2.2	2.0	4.7	2.7	14.8	14.4	18.9	8.7	22.4	34.6	33.6
CV (%)	19.5	2.9	23.3	26.3	26.2	60.2	37.4	39.1	59.0	86.1	53.4	54.1	25.4	33.9	24.9	24.5	24.3
19 years	29843.8	4.59	30.7	15.0	11.9	3.4	2.2	2.0	4.6	2.7	14.3	13.9	18.7	8.8	22.3	33.8	32.8

weighted mean concentrations over 19 years are also shown. The CV for rainfall was about 20%. The CVs for Na^+ (non-sea-salt [nss]), Mg^{2+}, Mg^{2+} (nss), Ca^{2+} and Ca^{2+} (nss) were greater than 50%, whereas the CVs for other ions were about 20–30%.

Figure 6 shows rainfall and volume-weighted average monthly concentrations of dissolved ions over 19 years. Total rainfall was highest in June and July. Volume-weighted average monthly concentrations of $[H^+]$ were almost constant, although there were slight decreases in May and June and slight increases in July and August. The yearly patterns of variation of $[H^+]$, $[NO_3^-]$ and $[NH_4^+]$ were similar. In summer (June, July, August and September) the pattern of variation of $[SO_4^{2-}]$ was similar to that of $[H^+]$. However, their patterns differed in winter and early spring (December, January, February, March and April). As acidification is mainly due to $[SO_4^{2-}]$ and $[NO_3^-]$ (Sicard et al., 2007), these results suggest that seasonal contributions of $[SO_4^{2-}]$ and $[NO_3^-]$ differ. Seasonal changes in $[SO_4^{2-}]$nss have been reported (Ohizumi T et al., 1997, Seto et al., 2002, 2004). The patterns of variation for $[Na^+]$ and $[Cl^-]$ were similar throughout the year, likely because most $[Na^+]$ and $[Cl^-]$ originated from sea-salt.

Rainfall and volume-weighted average monthly concentrations of dissolved ions over 19 years are summarized in Table 3. The arithmetic average and CV of each ion are also shown. CV for rainfall was about 40%, twice that of the CV for annual data. The CVs for Na^+, Na^+(nss) and Cl^- were each greater than 50%. The amount of sea-salt, including Na^+ and Cl^-, was greater in winter and smaller in summer. CVs for other ions were about 20–40%.

$[NO_3^-]$ / $[SO_4^{2-}]$nss ratio

Assessments of the $[NO_3^-]$ / $[SO_4^{2-}]$ nss ratio over time can show the relative contribution of these ions to acidity (Takahashi et al., 2000). Figure 7 shows yearly variations of this ratio (Fig. 7). Excluding the year 2001, the minimum ratio was 0.49 in 1991, with this ratio tending to increase gradually thereafter. The much lower ratio observed in 2001 may have been due to the eruption, on July 14, 2000, of Mount Oyama on Miyake-jima, an island in the Pacific Ocean located about 350 km east-southeast of Otsu. This eruption resulted in the

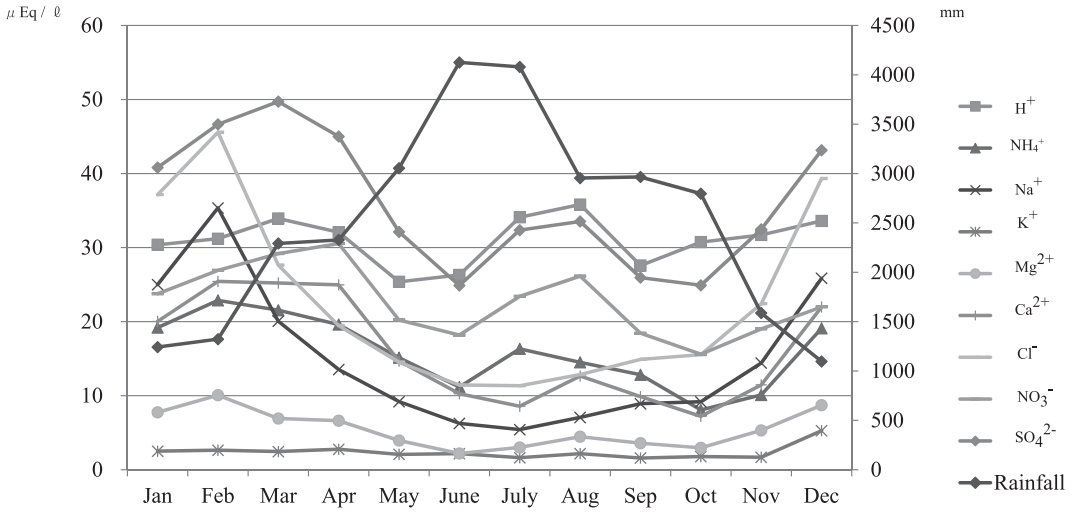

Fig. 6 Volume-weighted average monthly concentrations of H^+, NH_4^+, Na^+, K^+, Mg^{2+}, Ca^{2+}, Cl^-, NO_3^-, SO_4^{2-} and rainfall for 19 years

Table 3 Rainfall and volume-weighted average monthly concentrations of dissolved ion by months for 19 years (nss means non sea-salt)

	Rainfall (mm)	pH	H^+ (μEq/ℓ)	NH_4^+ (μEq/ℓ)	Na^+ (μEq/ℓ)	Na^+ (nss) (μEq/ℓ)	K^+ (μEq/ℓ)	K^+(nss) (μEq/ℓ)	Mg^{2+} (μEq/ℓ)	Mg^{2+} (nss) (μEq/ℓ)	Ca^{2+} (μEq/ℓ)	Ca^{2+} (nss) (μEq/ℓ)	Cl^- (μEq/ℓ)	Cl^-(nss) (μEq/ℓ)	NO_3^- (μEq/ℓ)	SO_4^{2-} (μEq/ℓ)	SO_4^{2-} (μEq/ℓ)
Jan	1244.3	4.60	30.4	19.2	25.0	6.4	2.5	2.1	7.8	3.6	20.0	19.2	37.1	15.7	23.8	40.8	38.6
Feb	1322.6	4.66	31.2	22.9	35.3	10.7	2.6	2.1	10.1	4.5	25.4	24.4	45.6	17.1	26.9	46.6	43.7
Mar	2295.2	4.60	33.9	21.5	20.1	5.0	2.4	2.1	6.9	3.5	25.2	24.6	27.6	10.2	29.2	49.7	47.9
Apr	2329.7	4.63	32.1	19.6	13.5	3.3	2.8	2.5	6.6	4.3	25.0	24.5	19.5	7.6	30.5	45.0	43.8
May	3142.0	4.63	25.4	15.1	9.2	2.5	2.1	1.9	3.9	2.4	14.7	14.4	14.5	6.8	20.2	32.1	31.3
June	4235.9	4.61	26.3	11.2	6.3	2.1	2.2	2.1	2.2	1.3	10.3	10.1	11.4	6.7	18.2	24.9	24.4
July	4080.3	4.52	34.1	16.3	5.4	2.3	1.6	1.6	3.0	2.3	8.6	8.4	11.3	7.7	23.4	32.4	32.0
Aug	2953.8	4.60	35.8	14.5	7.1	2.2	2.2	2.1	4.5	3.4	12.6	12.4	12.8	7.3	26.1	33.5	33.0
Sep	3050.5	4.60	27.6	12.8	8.9	3.0	1.6	1.5	3.6	2.3	9.9	9.6	14.9	8.1	18.4	25.9	25.2
Oct	2818.2	4.50	30.7	8.1	9.2	3.2	1.8	1.6	3.0	1.6	7.2	6.9	15.5	8.6	15.6	24.9	24.2
Nov	1653.5	4.51	31.7	10.1	14.4	3.6	1.7	1.5	5.3	2.9	11.5	11.0	22.4	9.9	19.0	32.5	31.2
Dec	1096.8	4.55	33.6	19.1	25.9	4.1	5.3	4.8	8.7	3.8	22.0	21.0	39.3	14.1	22.0	43.2	40.6
average	2518.6	4.59	31.1	15.9	15.0	4.0	2.4	2.2	5.5	3.0	16.0	15.5	22.7	10.0	22.8	36.0	34.7
CV (%)	40.1	1.1	10.0	28.5	60.7	58.0	39.8	39.9	44.3	33.0	42.0	41.7	50.5	34.8	19.8	23.4	22.5

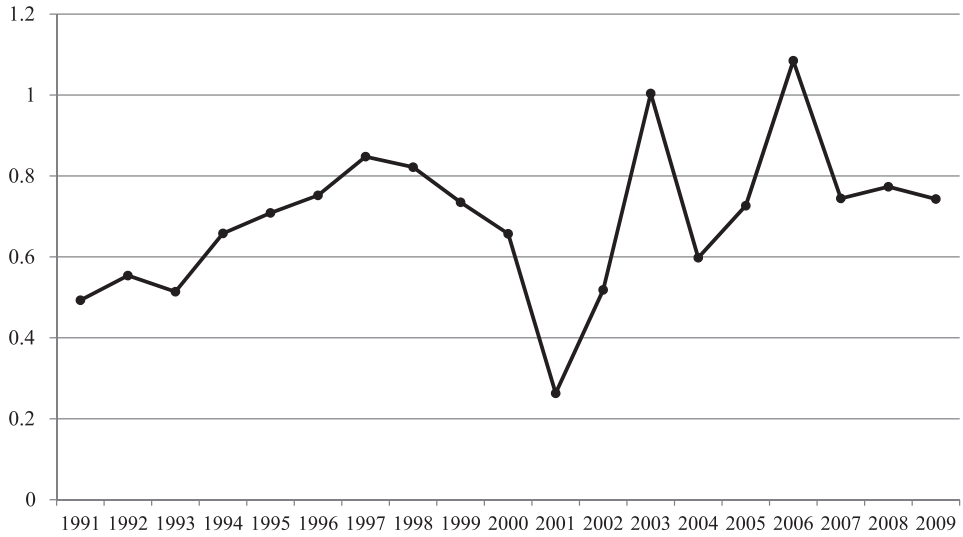

Fig. 7 Time series of $[NO_3^-]/[SO_4^{2-}]$ nss ratio. Volume-weighted annual mean concentrations are used.

emission of a large amount of SO_2 gas into the atmosphere. The $[NO_3^-]$ / $[SO_4^{2-}]$ nss ratio was reported to decrease from 1987 to 1996 (Takahashi et al., 2000), and $[SO_4^{2-}]$ nss was found to decrease from 1988 to 2002 at several sites in Japan (Noguchi et al., 2007).

Figure 8 shows the average monthly $[NO_3^-]$ / $[SO_4^{2-}]$ nss ratio over the 19 year study period. This ratio was high in summer, but lower in winter and early spring. The precipitation at Otsu seems to be influenced by both local and long-range sources. Seasonal changes show that the effects of SO_4^{2-} are greater than those of NO_3^- in winter and early spring, whereas the effects of NO_3^- are not negligible in summer. Other studies have also reported seasonal changes in the concentrations of sulfate and nitrate ions (Nakamura et al., 2009). As photochemical oxidation of NOx occurs more rapidly than that of SOx in the atmosphere, most SO_4^{2-} originates from long-range transferable sources (Ichikawa Y et al., 1995, Murano et al., 2000), whereas most NO_3^- originates from local sources of contamination, including exhaust from vehicles.

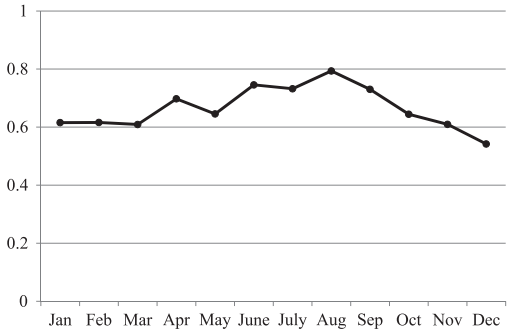

Fig. 8 $[NO_3^-]/[SO_4^{2-}]$ nss ratio of volume-weighted average monthly concentrations for 19 years.

Principal component analysis

The origin of dissolved ions was assessed by principal components analysis. The concentrations of dissolved ions in the 1818 samples were analyzed before sea-salt correction. The correlation matrix is shown in Table 4. We observed correlations >0.7 for Na^+ and Mg^{2+} (0.788), Na^+ and Cl^- (0.953), NH_4^+ and NO_3^- (0.764), NH_4^+ and SO_4^{2-} (0.730), Mg^{2+} and Ca^{2+} (0.746), Mg^{2+} and Cl^- (0.820), Ca^{2+} and SO_4^{2-} (0.761), and NO_3^- and SO_4^{2-} (0.773). Na^+, Cl^-, Mg^{2+} and Ca^{2+} correlated as sea-salts, whereas NO_3^-, SO_4^{2-} and NH_4^+ correlated as acidification and neutralization

Table 4 Correlation matrices of ion concentrations for 1818 samples.

	H^+	Na^+	NH_4^+	K^+	Mg^{2+}	Ca^{2+}	Cl^-	NO_3^-	SO_4^{2-}
H^+	1.000	0.036	0.371	0.072	0.076	0.059	0.107	0.542	0.53
Na^+		1.000	0.392	0.397	**0.788**	0.558	**0.953**	0.401	0.515
NH_4^+			1.000	0.492	0.469	0.510	0.415	**0.764**	**0.730**
K^+				1.000	0.439	0.431	0.417	0.444	0.427
Mg^{2+}					1.000	**0.746**	**0.820**	0.545	0.638
Ca^{2+}						1.000	0.530	0.667	**0.761**
Cl^-							1.000	0.395	0.493
NO_3^-								1.000	**0.773**
SO_4^{2-}									1.000

factors. Ca^{2+} may be correlated with SO_4^{2-} as a neutralizer in thermal power stations.

Diagonalization of the correlation matrix yielded nine eigenvectors (i. e. principal components). Principal components with larger eigenvalues are meaningful. Because the cumulative contributions of the first three principal components exceeded 80%, these three components were analyzed.

The eigenvalue of the first, second and third principal components were 5.1, 1.6 and 0.8, respectively, with these three principal components accounting for 83.5% of all eigenvalues. Figure 9 shows a plot of the factor loading values of the first versus the second principal component. All factor loading values of the first principal component were positive, making this component a good indicator of the contamination of precipitation samples (Mizukami et al. 1994). In the second principal component, the factor loading values of [NH_4^+], [NO_3^-] and [SO_4^{2-}] were negative and similar to each other (Group 1). In contrast, the factor loading value of [H^+], while negative, was very small, −0.74, and separate from the others. The factor loading values of [Cl^-], [Na^+] and [Mg^{2+}] were positive (Group 2), whereas [Ca^{2+}] and [K^+] had factor loading values < 0.1 (Group 3).

The second principal component indicates the origins of the dissolved ions. The ions in Group 1, which were important for acidification or neutralization of precipitation samples,

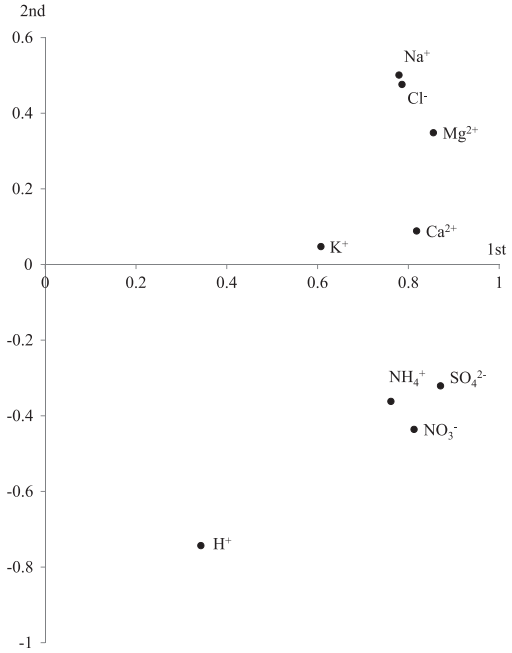

Fig. 9 Plots of the factor loading values of the first principal component vs. the second principal component.

originated from gas sources, such as SOx, NOx and NH_3. The ions in Group 2 ([Cl^-], [Na^+] and [Mg^{2+}]) originated from sea-salts. Of the ions in Group 3, [K^+] originated from soil, [Ca^{2+}] from both sea-salt and neutralization, and [H^+] from the balance between acidification and neutralization.

The factor loading values of the first principal component were plotted against those of the third principal component (Fig. 10). [Cl^-] and [Na^+] are close, because they originated from

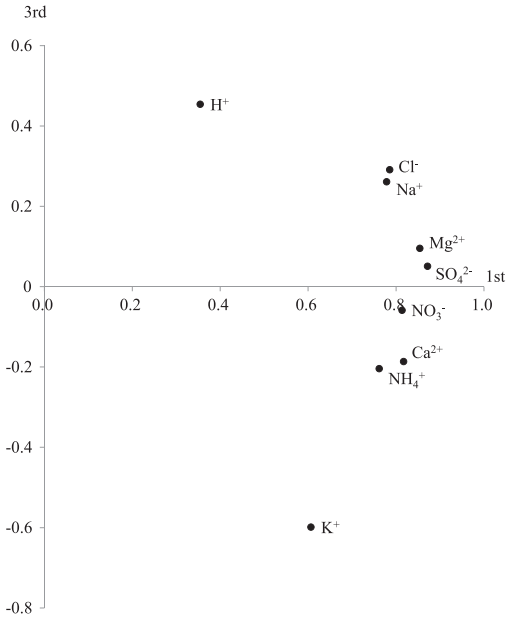

Fig. 10 Plots of the factor loading values of the first principal component vs. the third principal component.

sea-salts. The factor loading values of third principal component for [Mg^{2+}], [SO_4^{2-}], [NO_3^-], [Ca^{2+}] and [NH_4^+] were around zero. The latter four ions were associated with acidification and neutralization. [Mg^{2+}], which originated from sea-salts, was also slightly related to [SO_4^{2-}]. [K^+] and [H^+] were isolated, [K^+] because it originated from soil and [H^+] from the balance between acidification and neutralization.

Deposition according to rainfall

The frequency distribution of rainfall is shown in Fig. 11. Of the 1818 samples, over 500 were obtained from rainfall ≤5 mm. As rainfall increases, the number of samples decreases. Figure 11 also shows total ion deposition and cumulative ratio, as well as the depositions of the individual ions [H^+], [NO_3^-], [SO_4^{2-}], [NH_4^+], [Cl^-], [Na^+], [Mg^{2+}], [Ca^{2+}] and

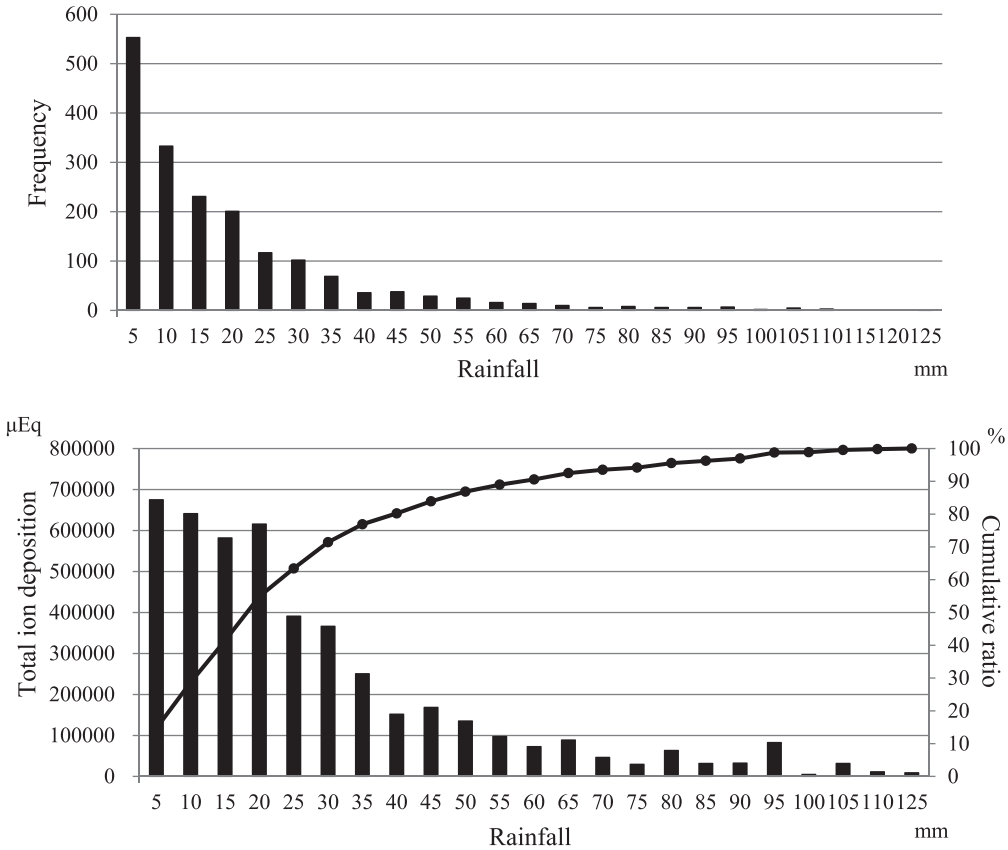

Fig. 11 Frequency distribution of rainfall and total ion deposition as a function of rainfall for 1818 samples.

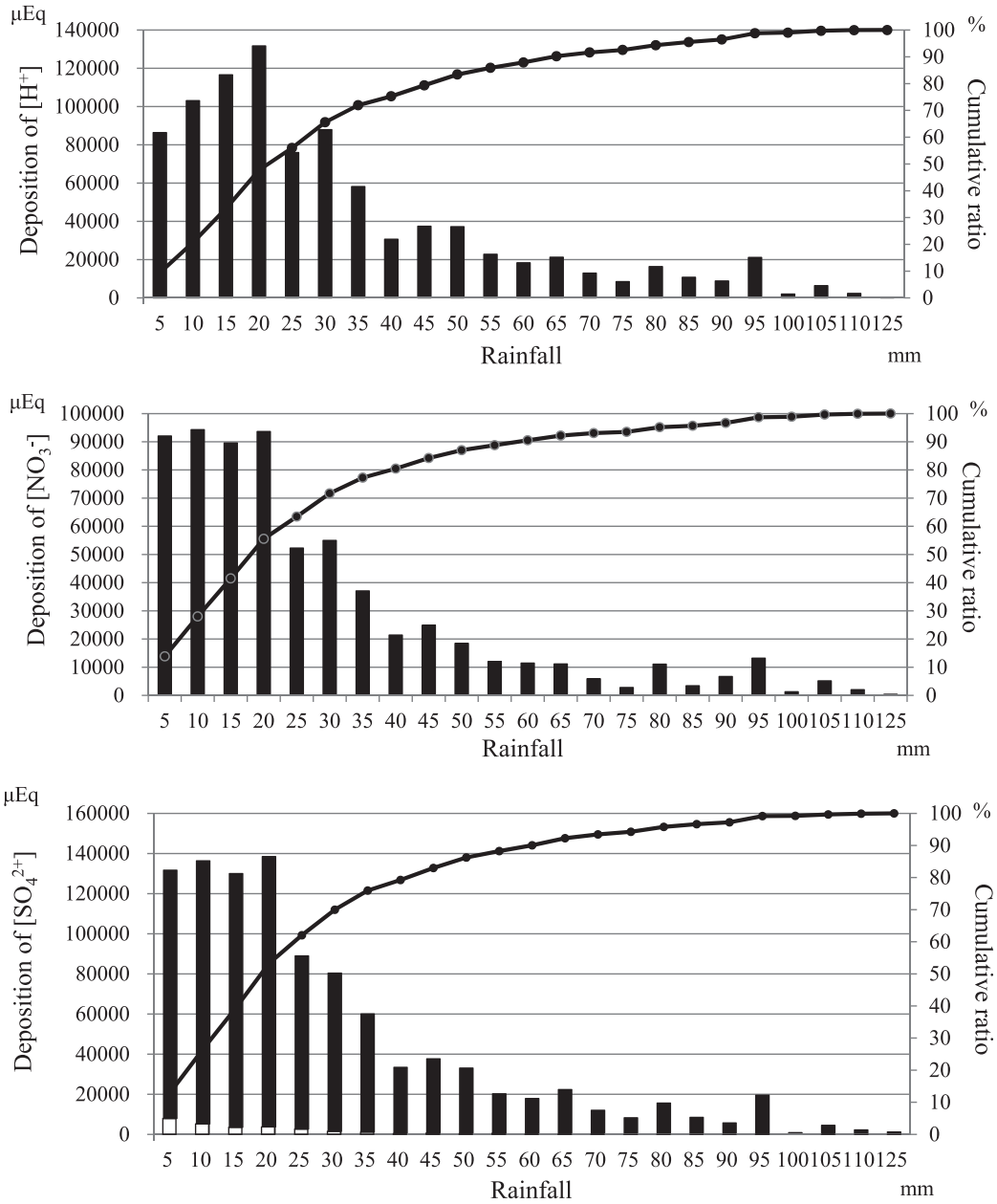

Fig. 11 (continued) Deposition of [H^+], [NO_3^-] and [SO_4^{2-}] as a function of rainfall for 1818 samples. White bar means deposition from sea-salt.

[K^+]. In Fig. 11 white bar means deposition from sea-salt. Total ion deposition showed peaks at 5 mm, 10 mm, 15 mm and 20 mm. At 25 mm, it decreased by about 30%, remaining similar at 30 mm. At 35 mm or more rainfall, ion deposition approximately decreased. Deposition of [H^+] tended to increase from 5 mm to 20 mm, decreasing by about 40% at 25 mm, increasing slightly at 30 mm and again decreasing at 35 mm. At 40 mm or more rainfall, [H^+] deposition is $<$40000 μEq.

[NO_3^-] and [SO_4^{2-}] are the dominant ions in acidification. The deposition of these ions as a function of rainfall shows patterns similar to

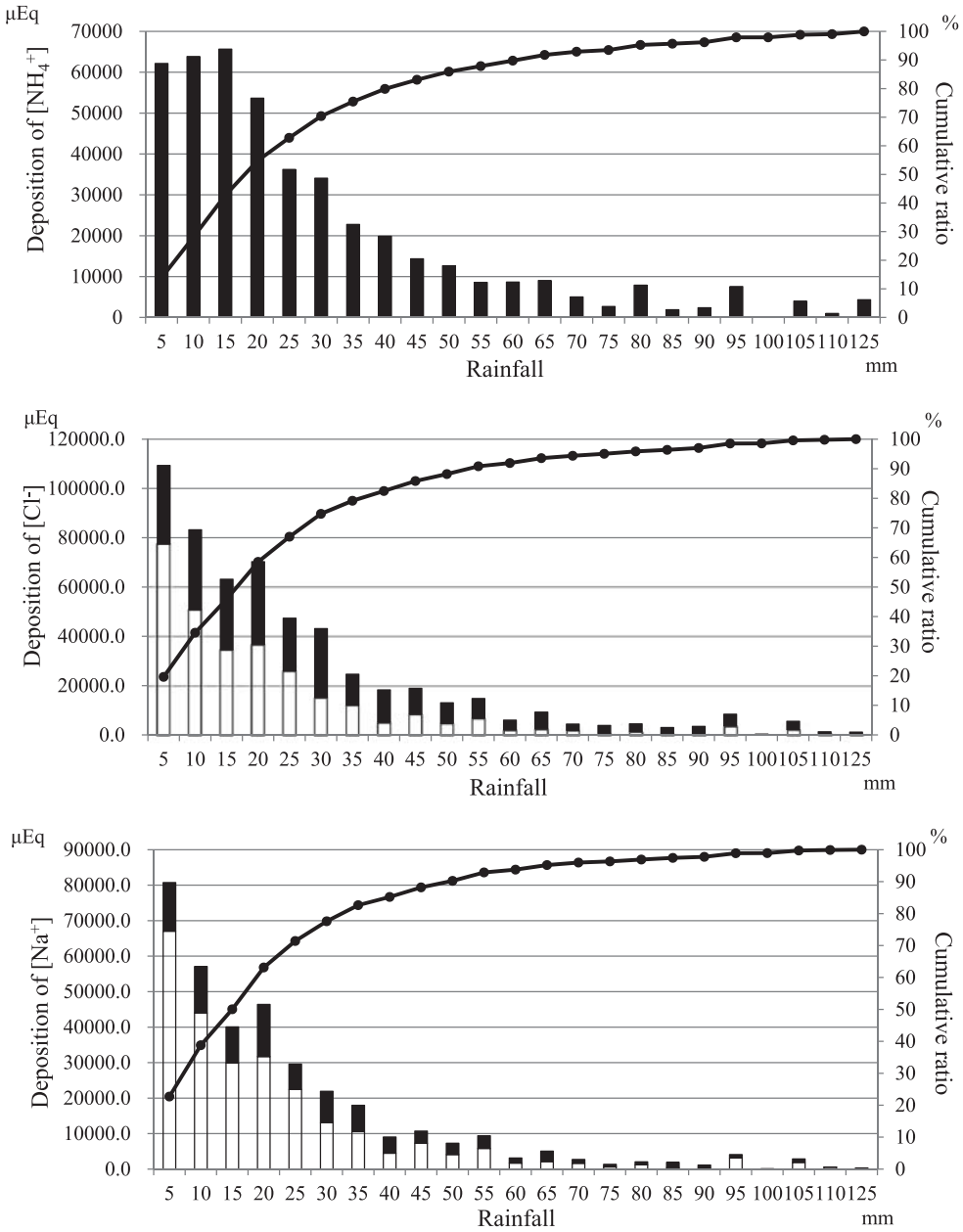

Fig. 11 (continued) Depositions of [NH_4^+], [Cl^-] and [Na^+] as a function of rainfall for 1818 samples. White bar means deposition from sea-salt.

that of total ion deposition. Most of the [SO_4^{2-}] does not derive from sea-salt. The deposition of [NH_4^+] is similar to those of [NO_3^-] and [SO_4^{2-}], except that [NH_4^+] decreases at 20 mm precipitation. The deposition of [Cl^-], [Na^+] and [Mg^{2+}] are similar to each other, with all three showing large contributions from sea-salt. Deposition of [Ca^{2+}] showed peaks at 5 mm and 10 mm, decreasing by about 30% at 15 mm, increasing slightly at 20 mm, and again decreasing above 25 mm. The deposition of [K^+] is the least among all ions tested. [K^+] peaked at 15 mm, decreasing gradually thereafter.

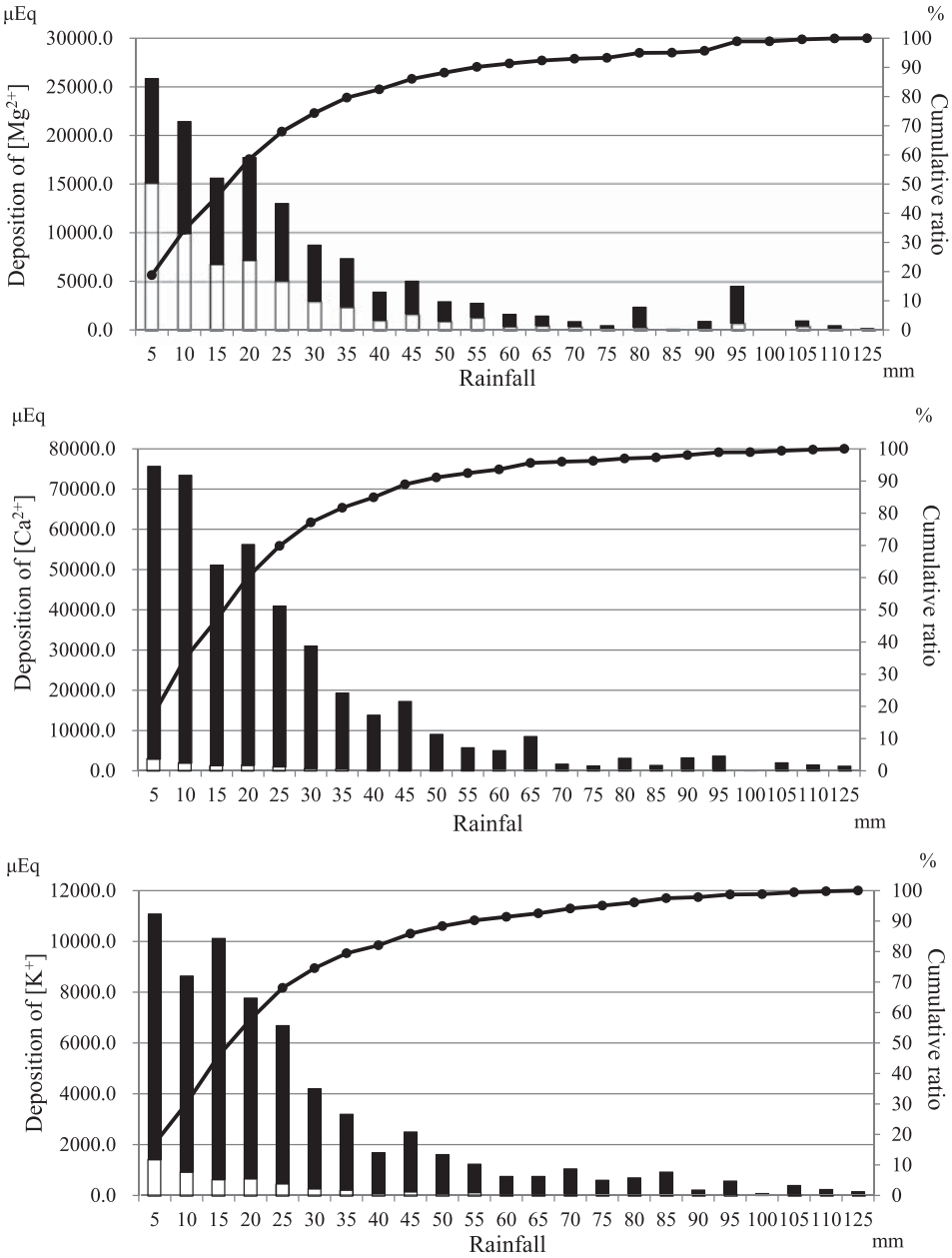

Fig. 11 (continued) Depositions of [Mg^{2+}], [Ca^{2+}] and [K^{+}] as a function of rainfall for 1818 samples. White bar means deposition from sea-salt.

Figure 12 shows the relationships between the deposition of [NO_3^-], [SO_4^{2-}], [NH_4^+], and [Ca^{2+}] as a function of rainfall, with deposition of [H^+] included for comparison. These patterns were very similar, strongly indicating that [NO_3^-] and [SO_4^{2-}] are acidification ions, whereas [NH_4^+] and [Ca^{2+}] are neutralization ions. Fig. 13 plots the deposition of [NO_3^-]+[SO_4^{2-}] versus that of [H^+]+[NH_4^+]+[Ca^{2+}] by months. The correlation was very good (slope, 1.02 ; R^2=0.953).

Blue-green algae are serious environmental problems in Lake Biwa. Typhoons supply considerable nutrients, which induce the growth of

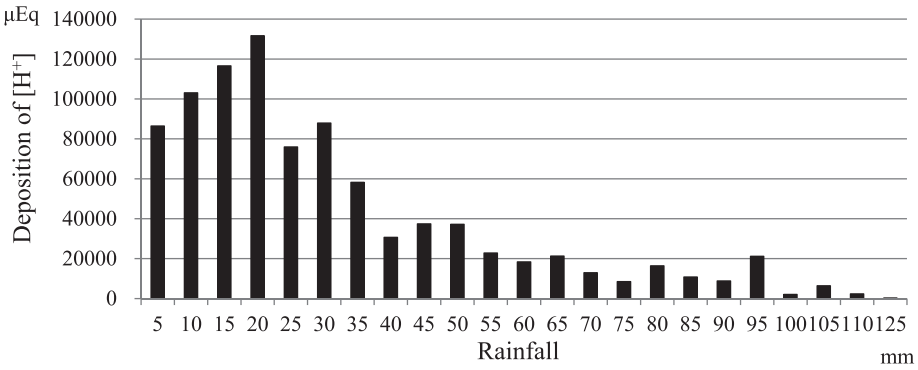

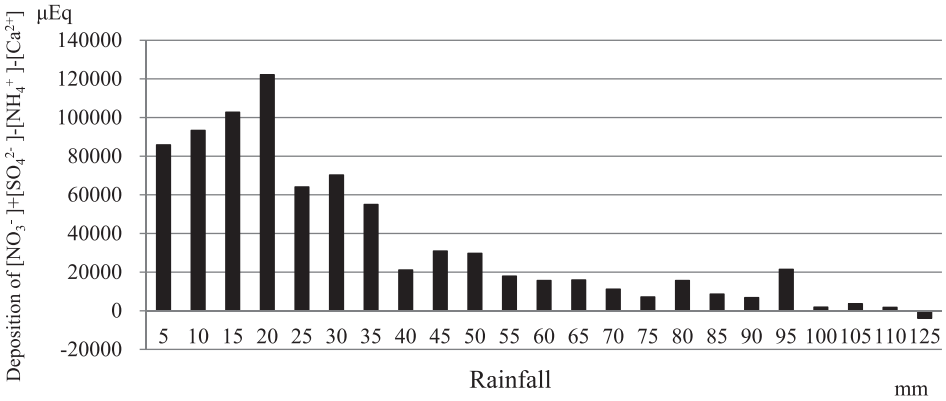

Fig. 12 Deposition of $[H^+]$ as a function of rainfall compared with those of $[NO_3^-]+[SO_4^{2-}]-[NHO_4^+]-[Ca^{2+}]$.

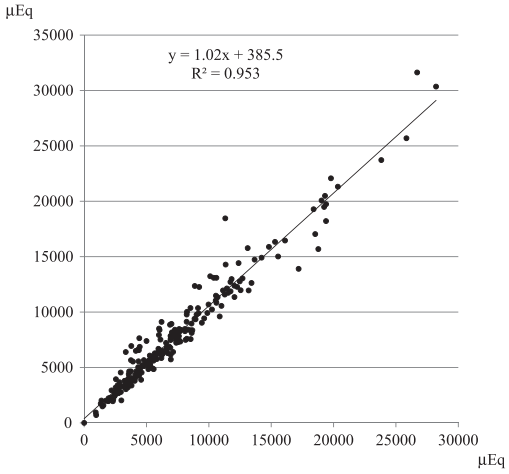

Fig. 13 Plots of depositions of $[NO_3^-]+[SO_4^{2-}]$ vs. depositions of $[H^+]+[NH_4^+]+[Ca^{2+}]$ by months

blue-green algae (Nalewajko et al. 2001). Another study focused on the effects of rain water on Lake Biwa, including the budget of dissolved trace metals originating from rain water (Mito et al., 2004; Mochizuki et al., 2016). Additional studies are needed to evaluate the relationships between weather and the concentration of dissolved ions.

In conclusion, this study showed trends of dissolved ion concentrations present in precipitation at Otsu over 19 years, from 1991 to 2009. The average pH of these samples was 4.59, with 86% of samples having a pH less than 5.0. The $[NO_3^-]/[SO_4^{2-}]$ nss ratio decreased sharply around 2001 because of the emission of SO_2 gas by a volcano in 2000. Principal component analysis suggests the origins of dissolved ions,

with [H^+] contributing to the balance between acidification and neutralization ions.

Acknowledgments We wish to thank all graduate and undergraduate students who supported this work.

References

Ichikawa Y, Fujita S (1995) An analysis of wet deposition of sulfate using a trajectory model for East Asia, Water Air Soil Pollut. 85 : 1927–1932.

Iida Y, Okamoto K, Ushio T (2006) Simulation of sampling error of average rainfall rate in space and time by five satellites using radar-AMeDAS composite, Geophys. Res. Lett. 33 : L01816.

Mito S, Sohrin Y, Norisuye K, Matsui M, Hasegawa H, Maruo M, Tsuchiya M, Kawashima M (2004) The budget of dissolved trace metals in Lake Biwa, Japan, Limnology 5 : 7–16.

Mizukami Y, Komori T, Kawashima M (1994) Chemical study of the precipitation by Lake Biwa at Otsu, Shiga, Japan. I. pH, dissolved ions and their sources, Jpn J Limnol 55 : 247–255.

Mochizuki A, Hosoda K, Sugiyama M (2016) Characteristic seasonal variation in dissolved uranium concentration induced by the change of lake water pH in Lake Biwa, Japan, Limnology 17 : 127–142.

Murano K, Mukai H, Hatakeyama S, Jang ES, Uno I (2000) Trans-boundary air pollution over remote islands in Japan : observed data and estimates from a numerical model, Atoms. Environ. 34 : 5139–5149.

Nakamura K, Mitani M (2009) Relationship between the monthly amount of wet deposition of sulfate and nitrate ions and the precipitation, Tenki 56 : 139–143 (in Japanese).

Nalewajko C, Murphy TP (2001) Effects of temperature, and availability of nitrogen and phosphorus on the abundance of Anabaena and Microcystis in Lake Biwa, Japan : an experimental approach, Limnology 2 : 45–48.

Noguchi I, Hayashi K, Aikawa M, Ohizumi T, Minami Y, Kitamura M, Takahashi A, Tanimoto H, Matsuda K, Hara H (2007) Temporal trends of non-sea salt sulfate and nitrate in wet deposition in Japan, Water Air Soil Pollut : Focus : 7 : 67–75.

Ohizumi T, Fukuzaki N (1997) Sulfur isotopic view on the sources of sulfur in atmospheric fallout along the coast of the sea of Japan, Atmos. Environ. 31 : 1339–1348.

Sicard P, Coddeville P, Sauvage S, Galloo J-C (2007) Trends in chemical composition of wet-only precipitation at rural French monitoring stations over the 1990–2003 period, Water Air Soil Pollut. : Focus 7 : 49–58.

Seto S, Nakamura A, Noguchi I, Ohizumi T, Fukuzaki N, Toyama S, Maeda M, Hayashi K, Hara H (2002) Annual and seasonal trends in chemical composition of precipitation in Japan during 1989–1998, Atmos. Environ. 36 : 3505–3517.

Seto S, Nakamura A, Hara H, Sato M, Noguchi I, Ohizumi T, Tonooka Y (2004) Annual and seasonal trends of wet deposition in Japan, Atmos. Environ. 38 : 3543–3556.

Takahashi A, Fujita S (2000) Long-term trends in nitrate to non-sea salt sulfate ratio in precipitation collected in western Japan, Atmos. Environ. 34 : 4551–4555.

要　旨

1991 年 1 月から 2009 年 12 月までの 19 年間にわたり、日本の滋賀県大津の琵琶湖のほとりで集められた雨のサンプルを分析した。1818 サンプルの溶存イオン、すなわち、水素イオン、アンモニウムイオン、ナトリウムイオン、カリウムイオン、カルシウムイオン、塩素イオン、硝酸イオン、硫酸イオンを分析した。これらのサンプルの水素イオン指数は 3.3 から 7.3 にわたり、平均値は 4.59 だった。主成分分析によって推測される溶存イオンの起源から 19 年間にわたる降水の化学成分の傾向が見出された。硝酸イオン、硫酸イオン、アンモニウムイオン、カルシウムイオンの間の負荷のバランスに依存して、水素イオンの負荷が特徴的な分布を示す。